

Bayesian Temporal Factorization for Multidimensional Time Series Prediction

Xinyu Chen, and Lijun Sun*,

Abstract—Large-scale and multidimensional spatiotemporal data sets are becoming ubiquitous in many real-world applications such as monitoring urban traffic and air quality. Making predictions on these time series has become a critical challenge due to not only the large-scale and high-dimensional nature but also the considerable amount of missing data. In this paper, we propose a Bayesian temporal factorization (BTF) framework for modeling multidimensional time series—in particular spatiotemporal data—in the presence of missing values. By integrating low-rank matrix/tensor factorization and vector autoregressive (VAR) process into a single probabilistic graphical model, this framework can characterize both global and local consistencies in large-scale time series data. The graphical model allows us to effectively perform probabilistic predictions and produce uncertainty estimates without imputing those missing values. We develop efficient Gibbs sampling algorithms for model inference and test the proposed BTF framework on several real-world spatiotemporal data sets for both missing data imputation and short-term/long-term rolling prediction tasks. The numerical experiments demonstrate the superiority of the proposed BTF approaches over many state-of-the-art techniques.

Index Terms—Time series analysis, missing data, matrix/tensor factorization, vector autoregression (VAR), Bayesian inference, Markov chain Monte Carlo (MCMC)



1 INTRODUCTION

With recent advances in sensing technologies, large-scale and multidimensional time series data—in particular spatiotemporal data—are collected on a continuous basis from various types of sensors and applications. Making predictions on these time series, such as forecasting urban traffic states and regional air quality, serves as a foundation to many real-world applications and benefits many scientific fields [1], [2]. For example, predicting the demand and states (e.g., speed, flow) of urban traffic is essential to a wide range of intelligent transportation systems (ITS) applications, such as trip planning, travel time estimation, route planning, traffic signal control, to name but a few [3]. However, given the complex spatiotemporal dependencies in these data sets, making efficient and reliable predictions for real-time applications has been a long-standing and fundamental research challenge.

Despite the vast body of literature on time series analysis from many scientific areas, three emerging issues in modern sensing technologies are constantly challenging the classical modeling frameworks. First, modern time series data are often large-scale, collected from a large number of subjects/locations/sensors simultaneously. For example, the highway traffic Performance Measurement System (PeMS) in California consists of more than 35,000 detectors, and it has been registering flow and speed information every 30 seconds since 1999 [4]. However, most classical

time series models are not scalable to handle large data sets. Second, modern time series generated by advanced sensing technologies are usually high-dimensional with different attributes. The multidimensional property makes it very difficult to characterize the higher-order correlations/dependencies together with the temporal dynamics across different dimensions in these time series data sets [5]. In addition to sensing data, multidimensional time series is also ubiquitous in social science domains such as international relations [6], dynamic import-export networks and social networks [7], and it is particularly important in modeling traffic/transportation systems with both origin and destination attributes. For example, mobility demand/flow for different types of travelers using different modes can be modeled as a 5-d (origin zone \times destination zone \times travel mode [e.g., car, transit, and bike] \times traveler type [e.g., child, adult, and senior] \times time) tensor time series and all dimensions have strong interactions with each other [8]. Third, most existing time series models require complete time series data as input, while in real-world sensor recordings the missing data problem is almost inevitable due to various factors such as hardware/software failure, human error, and network communication problems. Therefore, a critical challenge is to perform reliable prediction in the presence of missing data [9]. A simple solution is to adopt a two-stage approach: first applying imputation algorithms to fill in those missing entries, and then performing predictions based on the complete time series. This simple two-stage approach has been used in a wide range of real-world applications [10]; however, by applying imputation first, the prediction task actually suffers from accumulated errors resulted from the imputation algorithm.

To address these issues in modeling multivariate and multidimensional time series data, several notable approaches have been proposed recently based on ma-

- X. Chen and L. Sun are with the Department of Civil Engineering and Applied Mechanics, McGill University, Montreal, QC, H3A 0C3, Canada.
- L. Sun is also with the Interuniversity Research Center on Enterprise Network, Logistics and Transportation (CIRRELT), Montreal, QC, H3T 1J4, Canada.
- *Corresponding author. E-mail: lijun.sun@mcgill.ca

Manuscript received XXX; revised YYY.

trix/tensor factorization (see [1] for a brief review and e.g., [11], [12], [13], [14], [15], [16], [17], [18], [19], [20], [21], [22] for some representative models). As a common technique for collaborative filtering, matrix/tensor factorization presents a natural solution to address the scalability, efficiency, and missing data issues. Essentially, these models assume that the multivariate and multidimensional time series can be characterized by a low-rank structure with shared latent factors (i.e., global consistency). In order to create meaningful temporal patterns, different smoothing techniques and regularization schemes have been applied (e.g., linear dynamical systems [12] and Gaussian processes [15]) to impose local consistency. In a recent work, Yu *et al.* [19] proposed a Temporal Regularized Matrix Factorization (TRMF) framework to model multivariate time series with missing data by introducing a novel AR regularization scheme on the temporal factor matrix. This work is further extended in [20] to model spatiotemporal tensor data by introducing a spatial autoregressive regularizer, which enables us to perform predictions on the spatial dimension for unknown locations/sensors.

Overall, these factorization approaches have shown superior performance in modeling real-world large-scale time series data in the presence of missing values; however, there are still several main drawbacks hindering the application of these models. On the one hand, these models in general require careful tuning of the regularization parameters to ensure model accuracy and to avoid overfitting. The tuning procedure is computationally expensive and the cost increases exponentially with the number of parameters. Despite the computational cost, the tuning procedure has to be performed for each specific study/task/data set and there exist no universal solutions. On the other hand, these models essentially are not probabilistic and they can only provide point estimates of time series for prediction tasks. As a result, the reliability and uncertainty of the predictions are often overlooked. However, emerging real-world applications, such as route planning and travel time estimation, are extremely sensitive to uncertainties and risks.

In this paper, we propose a new Bayesian Temporal Factorization framework which can effectively handle both the missing data problem and high-dimensional property in modern spatiotemporal data. Our fundamental assumption is that these time series are highly correlated with shared latent factors. Inspired by the recent studies on temporal regularization [19] and Bayesian factorization [12], this framework applies low-rank matrix/tensor factorization to model multivariate and multidimensional spatiotemporal data and imposes a vector autoregressive (VAR) process to model the temporal factor matrix. The two components are integrated into a single probabilistic graphical model, on which we can design a fully Bayesian treatment. By placing conjugate prior over all parameters and hyperparameters, we can further develop efficient Markov chain Monte Carlo (MCMC) algorithms for model inference. The overall contribution of this framework is threefold:

- 1) We integrate VAR and matrix/tensor factorization into a single probabilistic framework to efficiently and effectively model large-scale and multidimensional (spatiotemporal) time series. This model can

impute missing values and predict future values simultaneously without introducing potential bias.

- 2) The framework is fully Bayesian and free from tuning regularization parameters, and thus it gives a flexible solution to ensure model accuracy and avoid overfitting. By using conjugate priors, we can derive efficient MCMC sampling algorithm for model inference. The Bayesian framework allows us to make probabilistic prediction with uncertainty estimates.
- 3) Extensive experiments are performed on real-world spatiotemporal data sets to demonstrate its effectiveness against state-of-the-art models.

The rest of this paper is organized as follows. In Section 2, we briefly review related work on modeling multivariate time series data and matrix/tensor factorization models for large-scale and multidimensional time series data. Section 3 provides a detailed description of the multivariate and multidimensional time series prediction problem in the presence of missing data. In Section 4, we present the Bayesian Temporal Matrix Factorization (BTMF) model for matrix time series data and develop an efficient MCMC algorithm for model inference. Section 5 extends BTMF to Bayesian Temporal Tensor Factorization (BTTF) to model tensor time series data. Section 6 provides the results on extensive numerical experiments based on several real-world data sets, followed by the conclusion and discussion in Section 7.

2 RELATED WORK

2.1 Traditional Multivariate and Multidimensional Time Series Models

Multivariate time series has been studied extensively in the literature. A classical approach is to consider the observations collected at a time point as a vector and model temporal dynamics using VAR process [23] and linear dynamical systems (LDS) [24]. Essentially, these models rely on using the AR coefficient matrix or the dynamics matrix to capture the correlation structure among different time series. Chen *et al.* [25] extended VAR model for matrix-valued time series data (i.e., a third-order tensor time series) by introducing two AR coefficient matrices to characterize the correlation structure. Despite the superior performance demonstrated by these models, the large number of parameters (in coefficient matrices) and the high computational cost make these models very difficult to estimate and prone to overfitting for large-scale problems. As a result, scalability becomes a key issue that limits the application of these models to small time series data set.

2.2 Matrix/Tensor Factorization for Time Series

While modeling large-scale time series is extremely challenging, it is also important to note that spatiotemporal data often exhibit high correlations and shared latent patterns (e.g., traffic state time series with repeated and reproducible temporal peaks). With this idea, many recent studies have proposed to apply matrix factorization (collaborative filtering) to analyze large-scale time series by projecting the raw data into a much smaller latent space.

In developing these factorization-based models, a central challenge is to design appropriate regularization terms to model temporal dynamics and smoothness, with the goal to both achieve high accuracy and avoid overfitting. For example, Chen and Cichocki [11] developed a non-negative matrix factorization model which temporal smoothness and spatial correlation regularizers. To address the scalability issue in LDS, Sun *et al.* [26] presented a dynamic matrix factorization (collaborative Kalman filtering) model for large-scale multivariate time series. Xie *et al.* [27] addressed the cold start problem in multivariate time series forecasting by high-dimensional regression with matrix factorization. Deng *et al.* [18] developed a latent space model for multivariate traffic state data on a transportation network with both missing values and missing sensors. Yu *et al.* [19] proposed to impose AR process to regularize the temporal factor matrix. Takeuchi *et al.* [20] extended [19] to model not only temporal dynamics but also spatial correlations in tensor data by introducing an additional graph Laplacian regularizer. Rogers *et al.* [13] proposed multilinear dynamical systems (MLDS) by integrating LDS and Tucker decomposition to model tensor time series data. Bahador *et al.* [14] developed a low-rank tensor learning method to efficiently learn patterns from multivariate spatiotemporal data. Cai *et al.* [17] developed a probabilistic temporal tensor decomposition model with not only temporal smoothing but also contextual constraints considered. Jing *et al.* [5] employed AR process constraints on the core tensor in Tucker decomposition. Harris *et al.* [28] proposed a low-rank method to estimate time-varying VAR model. Instead of imposing the low-rank assumption of the raw time series data or latent temporal factor matrix, the authors assume that the tensor composed by time-varying transition matrices follows a low-rank structure. Tan *et al.* [29] reorganized multivariate traffic time series data as a 4-d (sensor \times week \times day of week \times time of day) tensor to impute missing values. Although this approach does not model temporal smoothness explicitly, the factorization on the 4-d structure is able to learn repeated/reproducible temporal patterns (e.g., daily and weekly).

Essentially, these matrix/tensor factorization-based algorithms are scalable to model large-scale spatiotemporal data. In addition to uncovering latent temporal patterns (e.g., seasonality and trend) in multivariate time series data, these factorization models also serve as a powerful tool for collaborative filtering, thus offering a natural solution to deal with the missing data problem. However, in modeling the latent variables and temporal smoothness, these models have to introduce various regularization terms and parameters, which need to be tuned carefully to ensure model accuracy and avoid overfitting. The parameter tuning procedure is computationally very expensive and the cost increases exponentially with the number of regularization parameters as they have to be tuned simultaneously.

2.3 Bayesian Matrix/Tensor Factorization

Despite the parameter tuning problem, most of the factorization models above only provide point estimates for imputation/prediction tasks. This becomes a critical concern for real-world applications that are sensitive to uncertainties and risks. Since the introduction of Bayesian Probabilistic

Matrix Factorization (BPMF) [30], Bayesian treatment has been extensively implemented to address the overfitting and the parameter tuning problems in factorization models. For example, a Bayesian tensor factorization is proposed in [31], which can automatically determine the CP rank. Chen *et al.* [32] developed an augmented Bayesian tensor factorization model to estimate the posterior distribution of missing values in spatiotemporal traffic data. However, these models essentially focus on the global matrix/tensor factorization without explicitly modeling the local temporal and spatial dependencies in factor matrices (e.g., in [19], [20]). Xiong *et al.* [12] integrated a first-order dynamical structure to characterize temporal dependencies in Bayesian Gaussian tensor factorization. Charlin *et al.* [33] extended this model to dynamic Poisson matrix factorization for recommendation. The simple dynamical assumption imposes a smoothness constraint on the temporal factor matrix, thus the model can indeed better characterize the evolving dynamics of the data. However, the simple dynamical assumption does not have enough capability to characterize the complex dependencies for different lags, and thus limits its application for prediction tasks.

In this paper, we propose a novel Bayesian Temporal Factorization (BTF) framework that can simultaneously address the regularization parameter tuning problem and the uncertainty estimate problem in previous time series factorization models. As for BTMF, it can be considered the Bayesian counterpart of Yu *et al.* [19] by replacing the independent AR assumption on temporal factors with a more flexible VAR assumption. BTTF, on the other hand, can be considered an extension of the temporal collaborative filtering model by Xiong *et al.* [12] with a more powerful prediction mechanism.

3 PROBLEM DESCRIPTION

We assume a spatiotemporal setting for multidimensional time series data throughout this paper. In general, modern spatiotemporal data sets collected from sensor networks can be organized as matrix time series. For example, we can denote by matrix $Y \in \mathbb{R}^{N \times T}$ a multivariate time series collected from N locations/sensors on T time stamps, with each row

$$\mathbf{y}_i = (y_{i,1}, y_{i,2}, \dots, y_{i,t-1}, y_{i,t}, y_{i,t+1}, \dots, y_{i,T})$$

corresponding to the time series collected at location i . As another example, the time-varying origin-destination travel demand can be organized as a third-order time series tensor $\mathcal{Y} \in \mathbb{R}^{M \times N \times T}$ with M origin zones and N destination zones ($M = N$ in most cases), with each time series

$$\mathbf{y}_{i,j} = (y_{i,j,1}, y_{i,j,2}, \dots, y_{i,j,t-1}, y_{i,j,t}, y_{i,j,t+1}, \dots, y_{i,j,T})$$

showing the number of trips from i to j over time. Given the dimension/number of attributes collected from the underlying system, this formulation can be further extended to even higher-order tensors.

As mentioned, making accurate predictions on incomplete time series is very challenging, while missing data problem is almost inevitable in real-world applications. Figure 1 illustrates the prediction problem for incomplete time series data. Here we use $(i, t) \in \Omega$ and $(i, j, t) \in \Omega$

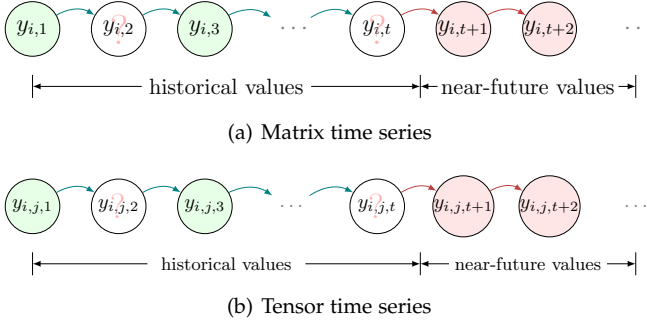


Fig. 1. Illustration of high-order time series and the prediction problem in the presence of missing values (green: observed data; white: missing data; red: prediction).

to index the observed entries in matrix Y and tensor \mathcal{Y} , respectively.

4 BAYESIAN TEMPORAL MATRIX FACTORIZATION

4.1 Model Specification

Given a partially observed matrix $Y \in \mathbb{R}^{N \times T}$ in a spatiotemporal setting, one can factorize it into a spatial factor matrix $W \in \mathbb{R}^{R \times N}$ and a temporal factor matrix $X \in \mathbb{R}^{R \times T}$ following general matrix factorization model:

$$Y \approx W^\top X, \quad (1)$$

and element-wise, we have

$$y_{i,t} \approx \mathbf{w}_i^\top \mathbf{x}_t, \quad \forall(i, t), \quad (2)$$

where vectors \mathbf{w}_i and \mathbf{x}_t refer to the i -th column of W and the t -th column of X , respectively.

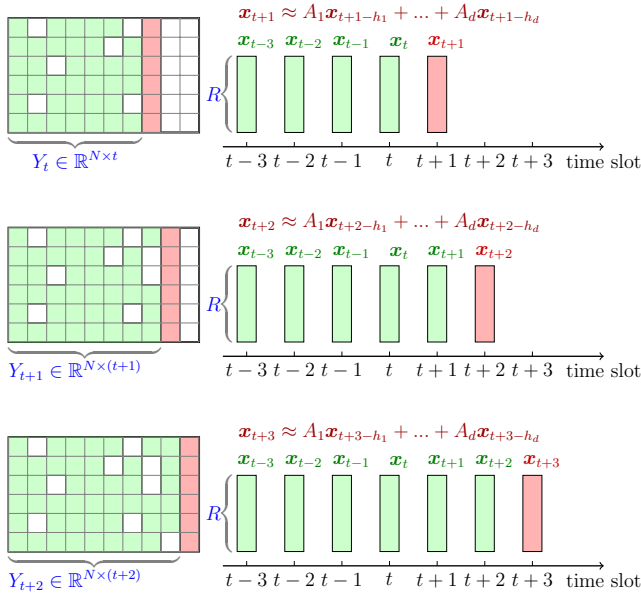


Fig. 2. A graphical illustration of the rolling prediction scheme using temporal matrix factorization (green: observed data; white: missing data; red: prediction).

The standard matrix factorization model is a good approach to deal with the missing data problem; however, it

cannot capture the temporal dependencies among different columns in X , which are critical in modeling time series data. To characterize the temporal dependencies, a VAR regularizer on X is introduced in TRMF [19]:

$$\mathbf{x}_{t+1} = \sum_{k=1}^d A_k \mathbf{x}_{t+1-h_k} + \epsilon_t, \quad (3)$$

where $\mathcal{L} = \{h_1, \dots, h_k, \dots, h_d\}$ is a lag set (d is the order of this AR model), each A_k ($k \in \{1, \dots, d\}$) is a $R \times R$ coefficient matrix, and ϵ_t is a zero mean Gaussian noise vector. In application, the coefficient matrix within AR regularizer is assumed to be a diagonal $A_k = \text{diag}(\theta_k)$ and thus factors are assumed to be independent:

$$\mathbf{x}_{t+1} = \theta_1 \otimes \mathbf{x}_{t+1-h_1} + \dots + \theta_d \otimes \mathbf{x}_{t+1-h_d} + \epsilon_t, \quad (4)$$

where the symbol \otimes denotes the element-wise Hadamard product. The VAR process can be used directly for prediction tasks. Given observed Y and a trained model, one can first predict $\hat{\mathbf{x}}_{t+1}$ on the latent temporal factor matrix X and then estimated time series data at $t+1$ with $y_{i,t+1} \approx \mathbf{w}_i^\top \hat{\mathbf{x}}_{t+1}$. Figure 2 illustrates a one-step rolling prediction scheme based on this idea. Therefore, by performing prediction on X instead of on Y , TRMF offers a scalable ($R \ll N$) and flexible scheme to model multivariate time series data.

However, in practice TRMF has two major limitations. First, although the independent factor assumption in (4) greatly reduces the number of parameters, the complex temporal dynamics, causal relationships and covariance structure are essentially overlooked. Second, TRMF requires careful tuning of multiple regularization parameters. The model may end up with overfitting if these regularization parameters are not tuned correctly. Despite existing parameter tuning solutions (e.g., cross-validation), it is still computationally very expensive to tuning multiple parameters simultaneously. Moreover, since there exist no universal/automatic solutions, this tuning procedure has to be done for each particular application (i.e., input data set).

To address the first limitation, in the proposed model we remove this diagonal constraint on A_k and employ the standard VAR process to characterize dynamic dependencies in X . For simplicity, we introduce matrix $A \in \mathbb{R}^{(Rd) \times R}$ and vector $\mathbf{v}_{t+1} \in \mathbb{R}^{(Rd) \times 1}$ as the form

$$A = [A_1, \dots, A_d]^\top, \quad \mathbf{v}_{t+1} = \begin{bmatrix} \mathbf{x}_{t+1-h_1} \\ \vdots \\ \mathbf{x}_{t+1-h_d} \end{bmatrix}$$

to summarize all coefficient matrices and correlated vectors. Therefore, we have $\mathbf{x}_{t+1} = A^\top \mathbf{v}_{t+1} + \epsilon_t$.

To address the second limitation, we propose the Bayesian Temporal Matrix Factorization (BTMF) model and extend it to multidimensional tensor time series. Most previous work on Bayesian temporal factorization essentially impose first-order Markovian/state-space assumptions on the temporal latent factor [12], [33]. These model may work well in temporal smoothing and pattern recognition, but the simple assumption limits its capacity in capturing complex time series dynamics and they cannot be applied directly for prediction tasks. We follow TRMF [19] and employ VAR process to characterize the temporal dependencies in X (see (3)), where VAR is indeed more flexible and its

Bayesian model [34]—BVAR—can be adapted to Bayesian matrix/tensor factorization naturally. Figure 3 shows the overall graphical representation of BTMF. Note that this model is entirely built on observed data in Ω and thus it can be trained on data sets with missing values. We next introduce each component in this graphical model in detail.

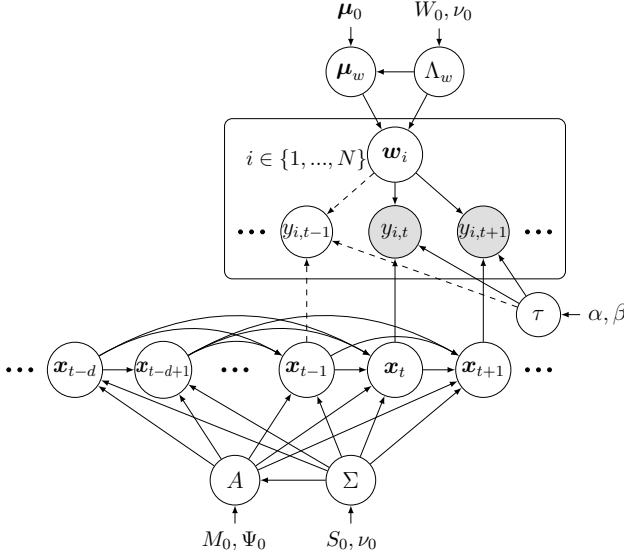


Fig. 3. An overview graphical model of BTMF (time lag set: $\{1, 2, \dots, d\}$). The shaded nodes $(y_{i,t})$ are the observed data in Ω .

Following the main idea of Bayesian probabilistic matrix/tensor factorization models (e.g., BPFM in [30] and BPTF in [12]), we assume that each observed entry in Y follows a Gaussian distribution with precision τ :

$$y_{i,t} \sim \mathcal{N}(w_i^\top x_t, \tau^{-1}), \quad (i, t) \in \Omega. \quad (5)$$

On the spatial factors, we use a simple Gaussian factor matrix without imposing any dependencies explicitly. The prior of vector w_i (i.e., i -th column of W) is a multivariate Gaussian distribution over μ_w and Λ_w :

$$w_i \sim \mathcal{N}(\mu_w, \Lambda_w^{-1}), \quad (6)$$

and we place a conjugate Gaussian-Wishart prior on the mean vector and the precision matrix:

$$\mu_w | \Lambda_w \sim \mathcal{N}(\mu_0, (\beta_0 \Lambda_w)^{-1}), \quad \Lambda_w \sim \mathcal{W}(W_0, \nu_0), \quad (7)$$

where $\mu_0 \in \mathbb{R}^R$ is a mean vector, $\mathcal{W}(W_0, \nu_0)$ is a Wishart distribution with a $R \times R$ scale matrix W_0 and ν_0 degrees of freedom.

In modeling the temporal factor matrix X , we re-write the VAR process as:

$$x_t \sim \begin{cases} \mathcal{N}(\mathbf{0}, I_R), & \text{if } t \in \{1, 2, \dots, h_d\}, \\ \mathcal{N}(A^\top v_t, \Sigma), & \text{otherwise,} \end{cases} \quad (8)$$

Since the mean vector is defined by VAR, we need to place the conjugate matrix normal inverse Wishart (MNIW) prior on the coefficient matrix A and the covariance matrix Σ as follows,

$$A \sim \mathcal{MN}_{(Rd) \times R}(M_0, \Psi_0, \Sigma), \quad \Sigma \sim \mathcal{IW}(S_0, \nu_0), \quad (9)$$

where the probability density function for the Rd -by- R random matrix A has the form:

$$\begin{aligned} p(A | M_0, \Psi_0, \Sigma) &= (2\pi)^{-R^2 d/2} |\Psi_0|^{-Rd/2} |\Sigma|^{-R/2} \\ &\times \exp\left(-\frac{1}{2} \text{tr}[\Psi_0^{-1} (A - M_0)^\top \Sigma^{-1} (A - M_0)]\right), \end{aligned} \quad (10)$$

where $\Psi_0 \in \mathbb{R}^{(Rd) \times (Rd)}$ and $\Sigma \in \mathbb{R}^{R \times R}$ are played as covariance matrices.

For the only remaining parameter τ , we place a Gamma prior $\tau \sim \text{Gamma}(\alpha, \beta)$ where α and β are the shape and rate parameters, respectively.

The above specifies the full generative process of BTMF. Several parameters are introduced to define the prior distributions for hyperparameters, including μ_0 , W_0 , ν_0 , β_0 , α , β , M_0 , Ψ_0 , and S_0 . These parameters need to be provided in advance when training the model. However, it should be noted that the specification of these parameters has little impact on the final results, as the training data will play a much more important role in defining the posteriors of the hyperparameters [12], [30].

4.2 Model Inference

Given the complex structure of BTMF, it is intractable to write down the posterior distribution. Here we rely on the MCMC technique for Bayesian learning. In detail, we introduce a Gibbs sampling algorithm by deriving the full conditional distributions for all parameters and hyperparameters. Thanks to the use of conjugate priors in Figure 3, we can actually write down all the conditional distributions analytically. Below we summarize the Gibbs sampling procedure.

Sampling (μ_w, Λ_w) . The conditional distribution is given by a Gaussian-Wishart:

$$p(\mu_w, \Lambda_w | -) = \mathcal{N}(\mu_w^*, ((\beta_0 + N) \Lambda_w)^{-1}) \times \mathcal{W}(W_w^*, \nu_w^*),$$

where

$$\begin{aligned} \mu_w^* &= \frac{1}{\beta_0 + N} (\beta_0 \mu_0 + N \bar{w}), \quad \nu_w^* = \nu_0 + N, \\ (W_w^*)^{-1} &= W_0^{-1} + N S_w + \frac{\beta_0 N}{\beta_0 + N} (\bar{w} - \mu_0) (\bar{w} - \mu_0)^\top, \\ \bar{w} &= \frac{1}{N} \sum_{i=1}^N w_i, \quad S_w = \frac{1}{N} \sum_{i=1}^N (w_i - \bar{w}) (w_i - \bar{w})^\top. \end{aligned}$$

Sampling (A, Σ) . Given the MNIW prior, the corresponding conditional distribution is

$$p(A, \Sigma | -) = \mathcal{MN}(M^*, \Psi^*, \Sigma) \times \mathcal{IW}(S^*, \nu^*), \quad (11)$$

and its parameters are given by:

$$\begin{aligned} \Psi^* &= (\Psi_0^{-1} + Q^\top Q)^{-1}, \\ M^* &= \Psi^* (\Psi_0^{-1} M_0 + Q^\top Z), \\ S^* &= S_0 + Z^\top Z + M_0^\top \Psi_0^{-1} M_0 - (M^*)^\top (\Psi^*)^{-1} M^*, \\ \nu^* &= \nu_0 + T - h_d, \end{aligned}$$

where the matrices $Z \in \mathbb{R}^{(T-h_d) \times R}$ and $Q \in \mathbb{R}^{(T-d) \times (Rd)}$ are defined as:

$$Z = \begin{bmatrix} \mathbf{x}_{h_d+1}^\top \\ \vdots \\ \mathbf{x}_T^\top \end{bmatrix}, \quad Q = \begin{bmatrix} \mathbf{v}_{h_d+1}^\top \\ \vdots \\ \mathbf{v}_T^\top \end{bmatrix}.$$

Sampling spatial factor \mathbf{w}_i . The conditional posterior distribution $p(\mathbf{w}_i | \mathbf{y}_i, X, \tau, \boldsymbol{\mu}_w, \Lambda_w)$ is a Gaussian distribution. Thus, we can sample $\mathbf{w}_i | - \sim \mathcal{N}(\boldsymbol{\mu}_w^*, (\Lambda_w^*)^{-1})$ with

$$\begin{aligned} \Lambda_w^* &= \tau \sum_{t:(i,t) \in \Omega} \mathbf{x}_t \mathbf{x}_t^\top + \Lambda_w, \\ \boldsymbol{\mu}_w^* &= (\Lambda_w^*)^{-1} \left(\tau \sum_{t:(i,t) \in \Omega} \mathbf{x}_t y_{i,t} + \Lambda_w \boldsymbol{\mu}_w \right). \end{aligned} \quad (12)$$

Sampling temporal factor \mathbf{x}_t . Given the VAR process, the conditional distribution of \mathbf{x}_t is also a Gaussian. However, for a particular time lag set, we need to define different updating rules for $1 \leq t \leq T - h_1$ and $T - h_1 < t \leq T$. Overall, the conditional distribution can be written as $p(\mathbf{x}_t | -) = \mathcal{N}(\boldsymbol{\mu}_t^*, \Sigma_t^*)$ with

$$\begin{aligned} \Sigma_t^* &= \left(\tau \sum_{i:(i,t) \in \Omega} \mathbf{w}_i \mathbf{w}_i^\top + M_t + P_t \right)^{-1}, \\ \boldsymbol{\mu}_t^* &= \Sigma_t^* \left(\tau \sum_{i:(i,t) \in \Omega} \mathbf{w}_i y_{i,t} + N_t + Q_t \right), \end{aligned} \quad (13)$$

where M_t and N_t are two auxiliary variables. In general cases where $1 \leq t \leq T - h_1$, we define M_t and N_t as follows:

$$\begin{aligned} M_t &= \sum_{k=1, h_d < t+h_k \leq T} A_k^\top \Sigma^{-1} A_k, \\ N_t &= \sum_{k=1, h_d < t+h_k \leq T} A_k^\top \Sigma^{-1} \boldsymbol{\psi}_{t+h_k}, \\ \boldsymbol{\psi}_{t+h_k} &= \mathbf{x}_{t+h_k} - \sum_{l=1, l \neq k}^d A_l \mathbf{x}_{t+h_k-h_l}. \end{aligned}$$

Otherwise, we define $M_t = 0$ and $N_t = 0$.

The variables P_t and Q_t in (13) are given by:

$$\begin{aligned} P_t &= \begin{cases} I_R, & \text{if } t \in \{1, 2, \dots, h_d\}, \\ \Sigma^{-1}, & \text{otherwise,} \end{cases} \\ Q_t &= \begin{cases} \mathbf{0}, & \text{if } t \in \{1, 2, \dots, h_d\}, \\ \Sigma^{-1} \sum_{l=1}^d A_l \mathbf{x}_{t-h_l}, & \text{otherwise.} \end{cases} \end{aligned}$$

Sampling precision τ . Given the conjugate Gamma prior, the conditional distribution of τ is also a Gamma distribution, i.e., we have $\tau | - \sim \text{Gamma}(\alpha^*, \beta^*)$ with $\alpha^* = \frac{1}{2} |\Omega| + \alpha$ and $\beta^* = \frac{1}{2} \sum_{(i,t) \in \Omega} (y_{i,t} - \mathbf{w}_i^\top \mathbf{x}_t)^2 + \beta$.

4.3 Model Implementation

4.3.1 Missing Data Imputation

Based on the aforementioned sampling processes, we summarize the the MCMC inference algorithm to impute missing values in the partially observed matrix time series data as Algorithm 1. In training the model, we first run the MCMC algorithm for m_1 iterations as a burn-in period and then take samples from the following m_2 iterations for estimation. Note that one can keep all the m_2 samples to get not only the mean but also the confidence interval for risk-sensitive applications.

Algorithm 1 BTMF-Gibbs sampling for imputation

Input: data matrix $Y \in \mathbb{R}^{N \times T}$, Ω as the set of observed entries in Y , $\mathcal{L} = \{h_1, h_2, \dots, h_d\}$ as the set of VAR lags, number of burn-in iterations m_1 , and number of samples used in estimation m_2 . Initialization of factor matrices $\{W, X\}$ and VAR coefficient matrix $A \in \mathbb{R}^{Rd \times R}$.

Output: estimated matrix $\hat{Y} \in \mathbb{R}^{N \times T}$.

Initialize $\beta_0 = 1$, $\nu_0 = R$, $\boldsymbol{\mu}_0 = \mathbf{0}$ as a zero vector, $W_0 = I_R$ ($S_0 = I_R$ and $\Psi_0 = I_{Rd}$) as an identity matrix, M_0 as all-zero mean matrix, and $\alpha, \beta = 10^{-6}$.

```

1: for iter. = 1 to  $m_1 + m_2$  do
2:   Draw hyperparameters  $\{\boldsymbol{\mu}_w, \Lambda_w\}$ .
3:   for  $i = 1$  to  $N$  do
4:     Draw  $\mathbf{w}_i \sim \mathcal{N}(\boldsymbol{\mu}_w^*, (\Lambda_w^*)^{-1})$ .
5:   end for
6:   Draw  $\Sigma \sim \mathcal{IW}(S^*, \nu^*)$  and  $A \sim \mathcal{MN}(M^*, \Psi^*, \Sigma)$ .
7:   for  $t = 1$  to  $T$  do
8:     Draw  $\mathbf{x}_t \sim \mathcal{N}(\boldsymbol{\mu}_t^*, \Sigma_t^*)$ .
9:   end for
10:  Draw precision  $\tau \sim \text{Gamma}(\alpha^*, \beta^*)$ .
11:  if iter. >  $m_1$  then
12:    Compute  $\tilde{Y} = W^\top X$ . Collect sample  $\tilde{Y}$ .
13:  end if
14: end for
15: return  $\hat{Y}$  as the average of the  $m_2$  samples of  $\tilde{Y}$ .

```

4.3.2 Rolling Spatiotemporal Prediction

To support multiple prediction applications, here we adapt Algorithm 1 for spatiotemporal prediction tasks and derive two BTMF implementation strategies. One is online implementation of BTMF for short-term prediction (e.g., single-step prediction). Another is used for long-term prediction (e.g., multi-step prediction). We next first describe the online rolling prediction task in detail (see Figure 2).

Assume that we have historical data $Y \in \mathbb{R}^{N \times t}$ and a trained model based on Y . The prediction task is to first have a good estimate of $\hat{\mathbf{y}}_{t+1}$ based on the trained model, and then estimate $\hat{\mathbf{y}}_{t+2}$ when \mathbf{y}_{t+1} —the actual observations at time point $t + 1$ —is available to us.

To make predictions efficiently, we keep W , X and A as fixed point estimates by averaging the m_2 samples of W , X , and A after training the model, and only consider \mathbf{x}_{t+1} as a new parameter to be updated over time [35]. We summarize the online BTMF prediction at each time point $t + 1$ as follows:

- Collect the actual observations of $\mathbf{y}_t \in \mathbb{R}^N$. Note that \mathbf{y}_t may contain missing values. Train a Bayesian model on \mathbf{y}_t as

$$\begin{aligned} y_{i,t} &\sim \mathcal{N}(\mathbf{w}_i^\top \mathbf{x}_t, \tau^{-1}), \quad i \in \Omega_t, \\ \mathbf{x}_t &\sim \mathcal{N}(A^\top \mathbf{v}_t, \Lambda_x^{-1}), \\ \tau &\sim \text{Gamma}(\alpha, \beta), \\ \Lambda_x &\sim \mathcal{W}(W_0, \nu_0), \end{aligned} \quad (14)$$

where Ω_t denotes the set of observed entries in vector \mathbf{y}_t , and vector $A^\top \mathbf{v}_t$ is—as defined in Eq. (8)—the mean vector of the multivariate Gaussian distribution of \mathbf{x}_t .

- Collect m_2 samples of $\tilde{\mathbf{y}}_{t+1} = W^\top A^\top \mathbf{v}_{t+1}$ (\mathbf{x}_{t+1} within \mathbf{v}_{t+1} is a new vector sample) in Gibbs sampling and average these m_2 samples as the predicted time series values $\hat{\mathbf{y}}_{t+1}$ at time $t + 1$. This finishes the prediction task. In the following we collect new data to update the model and prepare for the next prediction.

Here, the Gibbs algorithm to generate samples of \mathbf{x}_t is given by:

- 1) Draw hyperparameters $\Lambda_x \sim \mathcal{W}(W^*, \nu_0 + 1)$ with $(W^*)^{-1} = W_0^{-1} + (\mathbf{x}_t - A^\top \mathbf{v}_t)(\mathbf{x}_t - A^\top \mathbf{v}_t)^\top$.
- 2) Draw a new vector (sample) $\mathbf{x}_t \sim \mathcal{N}(\boldsymbol{\mu}_x^*, (\Lambda_x^*)^{-1})$ with

$$\Lambda_x^* = \tau \sum_{i \in \Omega_t} \mathbf{w}_i \mathbf{w}_i^\top + \Lambda_x,$$

$$\boldsymbol{\mu}_x^* = (\Lambda_x^*)^{-1} \left(\tau \sum_{i \in \Omega_t} \mathbf{w}_i y_{i,t} + \Lambda_x A^\top \mathbf{v}_t \right).$$
- 3) Draw $\tau \sim \text{Gamma}(\alpha^*, \beta^*)$ with $\alpha^* = \frac{1}{2}|\Omega_t| + \alpha$ and $\beta^* = \frac{1}{2} \sum_{i \in \Omega_t} (y_{i,t} - \mathbf{w}_i^\top \mathbf{x}_t)^2 + \beta$.

Since the Bayesian model has been trained using all available data, the MCMC algorithm for updating \mathbf{x}_t is expected to converge very fast in a few iterations and the m_2 samples can be generated very efficiently.

Again, we would like to emphasize that we only consider \mathbf{x}_t as a parameter to achieve high efficiency in this online prediction application. If we have enough computational power or if the Bayesian confidence interval of \mathbf{y}_t is of key consideration, we can easily design a fully Bayesian approach following Algorithm 1 to estimate the posterior distribution of \mathbf{y}_t (instead of a point estimate) by updating all the parameters—including W and A —in the Gibbs sampling algorithm. There are several ways to further reduce the computational cost. For example, during the Gibbs sampling, we can update parameter W and A using time series data collected from a shorter window (e.g., data collected from the last M time points ($M \ll t$)) instead of the whole data set.

Another rolling spatiotemporal prediction is the multi-step prediction which in this work is designed to make long-term prediction (e.g., forecast traffic in the next day). We summarize the BTMF at each time point t th iterate (i.e., forecast data with the time slots from $t \times T_0 + T_s + 1$ to $(t + 1) \times T_0 + T_s$ where T_0 is the number of time intervals per day and T_s is the start time slot) for this task as follows:

- Collect the actual observations $Y_{t \times T_0 + T_s}$ and train a BTMF model with m_1 burn-in iterations and m_2 iterations for sampling.
- Collect m_2 samples of W and $X_{t \times T_0 + T_s}$ and compute their averages, i.e., \hat{W} and $\hat{X}_{t \times T_0 + T_s}$, respectively.
- Estimate temporal factors with the time slots from $t \times T_0 + T_s + 1$ to $(t + 1) \times T_0 + T_s$ sequentially and derive predicted values $\hat{Y}_{(t+1) \times T_0 + T_s}$ by the multiplication $\hat{W} \times \hat{X}_{(t+1) \times T_0 + T_s}$.

To demonstrate the effectiveness of VAR, we also develop a Bayesian version of TRMF–BayesTRMF—as a baseline model. Note that BayesTRMF can be considered a special case of BTMF by employing the independent factor assumption in (4) instead of a VAR in (3).

5 BAYESIAN TEMPORAL TENSOR FACTORIZATION

It is straightforward to extend BTMF to model multidimensional (order > 2) tensor time series. We use a third-order tensor $\mathcal{Y} \in \mathbb{R}^{M \times N \times T}$ as an example throughout the section.

5.1 Model Specification

To model multidimensional data, we employ the popular CANDECOMP/PARAFAC (CP) decomposition [36], which approximates \mathcal{Y} by the sum of R rank-one tensors:

$$\mathcal{Y} \approx \sum_{r=1}^R \mathbf{u}_r \circ \mathbf{v}_r \circ \mathbf{x}_r, \quad (15)$$

where $\mathbf{u}_r \in \mathbb{R}^M$, $\mathbf{v}_r \in \mathbb{R}^N$, and $\mathbf{x}_r \in \mathbb{R}^T$ are the r -th column of factor matrices $U \in \mathbb{R}^{M \times R}$, $V \in \mathbb{R}^{N \times R}$, and $X \in \mathbb{R}^{T \times R}$, respectively (see Figure 4). The symbol \circ denotes vector outer product. Essentially, this model can be considered a high-order extension of (1).

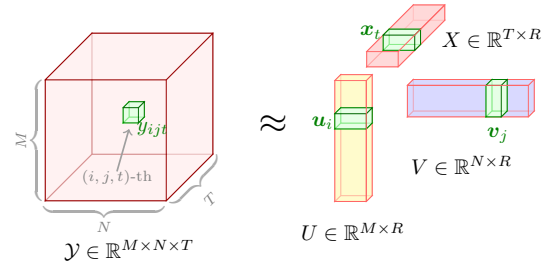


Fig. 4. A graphical illustration of CP factorization.

The CP decomposition provides us a natural way to extend BTMF to tensors by assuming that each element:

$$y_{i,j,t} \sim \mathcal{N} \left(\sum_{r=1}^R u_{ir} v_{jr} x_{tr}, \tau^{-1} \right), \quad (i, j, t) \in \Omega. \quad (16)$$

Following the same routine as BTMF, we define the generative process of Bayesian Temporal Tensor Factorization (BTTF) as follows:

$$\begin{aligned} \mathbf{u}_i &\sim \mathcal{N}(\boldsymbol{\mu}_u, \Lambda_u^{-1}), \\ \mathbf{v}_j &\sim \mathcal{N}(\boldsymbol{\mu}_v, \Lambda_v^{-1}), \\ \tau &\sim \text{Gamma}(\alpha, \beta), \end{aligned} \quad (17)$$

and in particular, the same VAR model in (8) can be used model temporal factor matrix X , and the prior is defined as:

$$\mathbf{x}_t \sim \begin{cases} \mathcal{N}(\mathbf{0}, I_R), & \text{if } t \in \{1, 2, \dots, h_d\}, \\ \mathcal{N}(A^\top \mathbf{v}_t, \Sigma), & \text{otherwise,} \end{cases} \quad (18)$$

where in this setting, the same Gaussian-Wishart priors as in BTMF can be placed for the underlying hyperparameters.

In BTTF, we may consider both U and V as spatial factor matrices, while in fact they may characterize any features in which dependencies are not explicitly encoded (e.g., type of travelers in [8] and type of sensors in [20]).

5.2 Model Inference

Section 4.2 has summarized the entire procedure of model inference for the parameters/hyperparameters in BTMF. Regarding posterior inference, the main difference between BTTF and BTMF is the posterior distribution of factor matrices. Specifically, the posterior distribution of \mathbf{x}_t in BTTF can be written as $p(\mathbf{x}_t|-) = \mathcal{N}(\boldsymbol{\mu}_t^*, \Sigma_t^*)$ with

$$\begin{aligned}\Sigma_t^* &= \left(\tau \sum_{i,j:(i,j,t) \in \Omega} \mathbf{w}_{ij} \mathbf{w}_{ij}^\top + M_t + P_t \right)^{-1}, \\ \boldsymbol{\mu}_t^* &= \Sigma_t^* \left(\tau \sum_{i,j:(i,j,t) \in \Omega} \mathbf{w}_{ij} y_{ijt} + N_t + Q_t \right),\end{aligned}\quad (19)$$

where $\mathbf{w}_{ij} = \mathbf{u}_i \otimes \mathbf{v}_j \in \mathbb{R}^R$, and $\{M_t, N_t, P_t, Q_t\}$ are defined in the same way as in BTMF (see (13)).

The posterior distribution of \mathbf{u}_i is $\mathcal{N}(\mathbf{u}_i | \boldsymbol{\mu}_i^*, (\Lambda_i^*)^{-1})$ with

$$\begin{aligned}\Lambda_u^* &= \tau \sum_{j,t:(i,j,t) \in \Omega} \mathbf{w}_{jt} \mathbf{w}_{jt}^\top + \Lambda_u, \\ \boldsymbol{\mu}_u^* &= (\Lambda_u^*)^{-1} \left(\tau \sum_{j,t:(i,j,t) \in \Omega} \mathbf{w}_{jt} y_{ijt} + \Lambda_u \boldsymbol{\mu}_u \right),\end{aligned}\quad (20)$$

where $\mathbf{w}_{jt} = \mathbf{v}_j \otimes \mathbf{x}_t \in \mathbb{R}^R$. The full conditional of \mathbf{v}_j is defined in the same way.

Under the assumptions above, the full conditionals $p(\boldsymbol{\mu}_u, \Lambda_u | -)$ and $p(\boldsymbol{\mu}_v, \Lambda_v | -)$ will be of the same Gaussian-Wishart form as $p(\boldsymbol{\mu}_w, \Lambda_w | -)$ described in BTMF. Similarly, the full conditional $p(A, \Sigma | -)$ is also of the same form as (11) in BTMF. For precision τ , the posterior Gamma distribution is given by $\text{Gamma}(\alpha^*, \beta^*)$ where $\alpha^* = \frac{1}{2} |\Omega| + \alpha$ and $\beta^* = \frac{1}{2} \sum_{(i,j,t) \in \Omega} (y_{i,j,t} - \sum_{r=1}^R u_{ir} v_{jr} x_{tr})^2 + \beta$.

5.3 Model Implementation

We summarize the Gibbs sampling algorithm for missing data imputation of BTTF as Algorithm 2.

6 EXPERIMENTS

In this section we apply BTMF and BTTF on several real-world spatiotemporal data sets for both imputation and prediction tasks, and evaluate the effectiveness of these two models against recent state-of-the-art approaches. We use the mean absolute percentage error (MAPE) and root mean square error (RMSE) as evaluation metrics:

$$\text{MAPE} = \frac{1}{n} \sum_{i=1}^n \frac{|y_i - \hat{y}_i|}{y_i} \times 100, \quad \text{RMSE} = \sqrt{\frac{1}{n} \sum_{i=1}^n (y_i - \hat{y}_i)^2},$$

where n is the total number of estimated values, and y_i and \hat{y}_i are the actual value and its estimation, respectively. For Bayesian algorithms, the point estimates are obtained by averaging over $m_2 = 100$ Gibbs iterations. The code and adapted data sets for our experiments are available at <https://github.com/xinychen/transdim>.

Algorithm 2 BTTF-Gibbs sampling for imputation

Input: data tensor $\mathcal{Y} \in \mathbb{R}^{M \times N \times T}$, Ω as the set of observed entries in \mathcal{Y} , $\mathcal{L} = \{h_1, h_2, \dots, h_d\}$ as the set of AR lags, number of burn-in iterations m_1 , and number of samples used in estimation m_2 . Initialization of factor matrices $\{U, V, X\}$ and VAR coefficient matrix $A \in \mathbb{R}^{Rd \times R}$.

Output: estimated tensor $\hat{\mathcal{Y}} \in \mathbb{R}^{M \times N \times T}$.

Initialize $\beta_0 = 1$, $\nu_0 = R$, $\boldsymbol{\mu}_0 = \mathbf{0}$ as a zero vector, $W_0 = I_R$ ($S_0 = I_R$ and $\Psi_0 = I_{Rd}$) as an identity matrix, M_0 as all-zero mean matrix, and $\alpha, \beta = 10^{-6}$.

- 1: **for** iter. = 1 to $m_1 + m_2$ **do**
- 2: Draw hyperparameters $\{\boldsymbol{\mu}_u, \Lambda_u, \boldsymbol{\mu}_v, \Lambda_v\}$.
- 3: **for** $i = 1$ to M **do**
- 4: Draw $\mathbf{u}_i \sim \mathcal{N}(\boldsymbol{\mu}_u^*, (\Lambda_u^*)^{-1})$.
- 5: **end for**
- 6: **for** $j = 1$ to N **do**
- 7: Draw $\mathbf{v}_j \sim \mathcal{N}(\boldsymbol{\mu}_v^*, (\Lambda_v^*)^{-1})$.
- 8: **end for**
- 9: Draw $\Sigma \sim \mathcal{IW}(S^*, \nu^*)$ and $A \sim \mathcal{MN}(M^*, \Psi^*, \Sigma)$.
- 10: **for** $t = 1$ to T **do**
- 11: Draw $\mathbf{x}_t \sim \mathcal{N}(\boldsymbol{\mu}_t^*, \Sigma_t^*)$.
- 12: **end for**
- 13: Draw precision $\tau \sim \text{Gamma}(\alpha^*, \beta^*)$.
- 14: **if** iter. $> m_1$ **then**
- 15: Compute $\tilde{\mathcal{Y}} = \sum_{r=1}^R \mathbf{u}_r \circ \mathbf{v}_r \circ \mathbf{x}_r$. Collect sample $\tilde{\mathcal{Y}}$.
- 16: **end if**
- 17: **end for**
- 18: **return** $\hat{\mathcal{Y}}$ as the average of the m_2 samples of $\tilde{\mathcal{Y}}$.

6.1 BTMF

Data set (G): Guangzhou urban traffic speed¹. This data set registered traffic speed data from 214 road segments over two months (61 days from August 1 to September 30, 2016) with a 10-minute resolution (144 time intervals per day) in Guangzhou, China. We organize the raw data set into a time series matrix of 214×8784 and there are 1.29% missing values.

Data set (B): Birmingham parking². This data set registered occupancy (i.e., number of parked vehicles) of 30 car parks in Birmingham City for every half an hour between 8:00 and 17:00 over more than two months (77 days from October 4, 2016 to December 19, 2016). The size of this time series matrix is 30×1386 with 18 time intervals per day and the amount of missing values is 14.89% after data processing. In particular, the data is completely missing on four days (October 20/21 and December 6/7).

Data set (H): Hangzhou metro passenger flow³. This data set collected incoming passenger flow from 80 metro stations over 25 days (from January 1 to January 25, 2019) with a 10-minute resolution in Hangzhou, China. We discard the interval 0:00 a.m. – 6:00 a.m. with no services (i.e., only consider the remaining 108 time intervals) and re-organize the raw data set into a time series matrix of 80×2700 .

Data set (S): Seattle freeway traffic speed⁴. This data set

1. <https://doi.org/10.5281/zenodo.1205229>
2. <https://archive.ics.uci.edu/ml/datasets/Parking+Birmingham>
3. <https://tianchi.aliyun.com/competition/entrance/231708/information>
4. <https://github.com/zhiyongc/Seattle-Loop-Data>

TABLE 1
Performance comparison for RM and NM for imputation tasks on data sets (G), (B), (H), and (S).

	BTMF	BayesTRMF	TRMF	BPMF	BGCP	BATF	HaLRTC	TF-ALS
20%, RM-G	7.47/3.19	7.37/3.14	7.47/3.14	9.54/4.06	8.28/3.57	8.32/3.59	8.15/3.33	8.33/3.59
40%, RM-G	7.81/3.35	7.56/3.24	7.76/3.25	9.81/4.17	8.29/3.59	8.36/3.61	8.87/3.61	8.37/3.62
20%, NM-G	10.16/4.27	10.21/4.27	10.24/4.27	10.28/4.29	10.20/4.27	10.17/4.26	10.46/ 4.21	10.27/4.30
40%, NM-G	10.36/4.46	10.43/4.50	10.37/4.37	10.40/4.40	10.25/4.32	10.17/4.30	10.88/4.38	10.28/4.33
10%, RM-B	1.71/7.44	1.64/6.40	2.77/10.57	7.87/81.59	6.50/19.69	6.93/20.65	4.85/17.35	6.15/18.50
30%, RM-B	2.61/ 13.38	2.31/13.77	3.69/21.80	9.95/83.82	6.23/19.98	6.68/21.29	6.64/26.79	5.83/18.91
10%, NM-B	12.05/28.27	12.10/ 28.18	12.74/29.46	13.18/29.28	13.64/43.15	16.28/40.81	9.47/34.72	14.47/41.67
30%, NM-B	15.44/61.69	15.10/59.66	16.35/85.98	14.75/60.29	15.93/ 57.07	15.95/ 57.07	14.83/92.59	17.65/63.85
20%, RM-H	25.18/ 28.51	22.40/30.32	21.31/37.07	29.63/41.87	19.01/41.16	22.74/33.07	18.26/28.88	19.91/111.30
40%, RM-H	26.83/32.19	23.87/32.73	22.89/38.15	32.83/44.46	19.59/32.71	23.17/ 31.62	19.01/31.81	20.98/100.32
20%, NM-H	26.50/81.73	26.80/74.27	26.07/40.06	36.31/64.28	25.57/35.99	34.94/ 29.32	20.29/40.53	28.37/42.61
40%, NM-H	30.24/80.53	28.13/71.87	27.32/39.75	36.43/59.04	24.37/49.64	30.63/48.01	21.47/53.26	28.11/ 38.42
20%, RM-S	5.92/3.71	5.92/3.71	5.96/3.71	6.51/4.04	7.45/4.50	8.70/3.73	5.95/ 3.48	7.42/4.49
40%, RM-S	6.18/3.79	6.18/3.79	6.16/3.79	7.03/4.29	7.58/4.54	8.73/ 3.75	6.77/3.84	7.58/4.56
20%, NM-S	9.12/5.27	9.12/5.28	9.12/5.26	9.12/5.27	9.93/5.65	10.15/ 4.25	8.82/4.70	9.95/5.63
40%, NM-S	9.20/5.33	9.21/5.33	9.19/5.30	9.19/5.30	9.94/5.68	10.15/ 4.30	10.20/5.28	10.04/5.70

Best results are highlighted in bold fonts.

TABLE 2
Performance comparison for RM and NM for prediction tasks on data sets (G), (B), (H) and (S).

	Single-step prediction			Multi-step prediction		
	BTMF	BayesTRMF	TRMF	BTMF	BayesTRMF	TRMF
Original G	10.25/4.09	10.70/4.27	10.65/4.30	13.40/5.10	17.03/6.37	15.57/5.86
20%, RM-G	10.45/4.17	11.03/4.43	10.62/4.31	13.36/5.08	18.78/7.10	15.78/5.91
40%, RM-G	10.78/4.31	11.19/4.49	10.62/4.30	13.58/5.17	18.01/6.68	15.78/5.86
20%, NM-G	10.67/ 4.27	11.12/4.49	10.64/4.29	13.59/5.16	19.15/7.44	15.40/5.73
40%, NM-G	11.32/4.59	11.97/4.91	10.71/4.32	13.68/5.21	20.94/8.16	16.06/5.99
Original B	25.10/155.32	31.80/161.11	32.63/174.25	19.89/183.29	34.49/292.10	27.78/230.43
10%, RM-B	23.55/127.45	32.07/167.16	32.67/171.69	23.70/168.61	40.37/339.97	27.55/213.01
30%, RM-B	22.79/131.60	31.21/166.87	34.42/181.17	20.23/168.35	26.04/183.63	34.07/225.04
10%, NM-B	24.28/142.45	33.00/170.48	31.95/169.30	19.28/156.69	38.60/326.77	26.93/252.05
30%, NM-B	23.60/138.72	35.71/173.65	33.09/175.64	27.65/ 173.34	35.53/276.11	26.88/192.53
Original H	30.04/ 37.29	30.17/40.87	27.77/39.99	38.84/41.03	40.54/46.84	24.76/39.96
20%, RM-H	29.38/ 38.28	32.34/48.20	27.59/40.73	37.50/40.59	30.09/41.31	24.93/38.36
40%, RM-H	30.49/ 39.96	34.93/49.30	26.68/47.80	38.93/40.94	31.31/43.39	26.09/39.62
20%, NM-H	30.26/46.62	30.85/49.20	26.58/45.23	44.67/54.27	33.82/51.80	23.29/39.89
40%, NM-H	30.52/45.89	29.69/51.64	28.78/41.02	37.62/56.24	41.20/59.56	25.83/44.45
Original S	7.48/4.54	7.90/4.78	7.96/4.90	15.64/8.47	24.25/13.31	19.10/9.93
20%, RM-S	7.64/4.61	8.13/4.90	7.95/4.90	15.90/8.62	21.18/11.41	18.99/10.10
40%, RM-S	7.85/4.72	8.41/5.08	7.95/4.90	15.49/8.47	19.80/10.48	17.85/9.45
20%, NM-S	7.69/4.65	7.96/4.84	7.94/4.89	16.40/8.90	23.70/12.87	18.41/9.70
40%, NM-S	7.98/4.83	8.47/5.12	7.96/4.90	16.84/9.15	23.23/12.58	17.10/9.08

Best results are highlighted in bold fonts.

collected freeway traffic speed from 323 loop detectors with a 5-minute resolution over the whole year of 2015 in Seattle, USA. We choose the data from January 1 to January 28 (i.e., 4 weeks) as our experiment data, and organize the data set into a time series matrix of 323×8064 .

Baselines. We choose 1) TRMF [19] and 2) its fully Bayesian counterpart—BayesTRMF—as main benchmark models. We also consider a family of tensor-based models for missing data imputation, including: 3) Bayesian Gaussian CP decomposition (BGCP) [37], which is a high-order extension of BPMF [30]; 4) Bayesian Augmented Tensor Factorization (BATF) [32]; 5) HaLRTC: High-accuracy Low-Rank Tensor Completion [38]; 6) TF-ALS: standard tensor factorization using Alternating Least Square (ALS). These models are chosen because matrix time series data collected from multiple days can be re-organized as a third-order (location \times day \times time of day) tensor, and in this case ten-

sor factorization can effectively learn the global patterns provided by the additional “day” dimension. In fact, these tensor models have shown superior performance in various imputation tasks (e.g., traffic data and images). For prediction, we compare BTMF against TRMF and BayesTRMF. In doing so, we adapt TRMF/BayesTRMF to an online implementation similar to (online) BTMF.

Experiment setup. We assess the performance of these models under two common missing data scenarios—random missing (RM) and non-random missing (NM). For RM, we simply remove a certain amount of observed entries in the matrix randomly and use these entries as ground truth to evaluate MAPE and RMSE. The percentages of missing values are set as 20% and 40% for data set (G), (H), and (S), and 10% and 30% for (B), respectively. For NM, we apply a fiber/block missing experiment by randomly choosing certain location \times day combinations and removing the

all observations in each combination. Again, the removed but actually observed entries are used for evaluation. The NM scenario corresponds to cases where sensors have a certain probability to fail on each day. For tensor-based baseline models (BGCP, BATE, HaLRTC, and TF-ALS), we reorganize the matrix into a third-order (location \times day \times time slot) tensor as input. For matrix based models, we use the original time series matrix (location \times time series) as input. For BTMF, BayesTRMF and TRMF, we use a small lag set $\mathcal{L} = \{1, 2, T_0\}$ for all data sets, where T_0 denotes the number of time intervals per day.

For the prediction tasks, we first apply a short-term rolling prediction experiment (e.g., single-step rolling prediction) as described in Figure 2 and Section 4.3, then, we conduct a multi-step predict experiment where we evaluate the next-day prediction. We evaluate these models by making rolling predictions over the last five days (i.e., 5×144 time slots) for data set (G), the last seven days (i.e., 7×18 time slots) for data set (B), the last five days (i.e., 5×108 time slots) for data set (H), and the last five days (i.e., 5×288 time slots) for data set (S). We apply the same sets of time lags $\mathcal{L} = \{1, 2, T_0\}$ as in the imputation experiments for the single-step prediction task. To guarantee the models' performance on multi-step prediction tasks, we set time lags as $\mathcal{L} = \{1, 2, 3, T_0, T_0+1, T_0+2, 7T_0, 7T_0+1, 7T_0+2\}$. Note that BTMF, BayesTRMF and TRMF will not impute missing values for these prediction tasks.

Results and analysis. We evaluate the proposed BTMF model on both imputation and prediction tasks. For the imputation experiment, TRMF and tensor completion models are main benchmark models.

Table 1 shows the imputation performance of BTMF and other baselines for data sets (G), (B), (H), and (S). The results in all experiments are given by "MAPE/RMSE". As can be seen, the proposed BTMF and the adapted BayesTRMF clearly outperform the TRMF in most of the cases. The results reveal that Bayesian treatment over temporal matrix factorization is more superior than manually controlling those regularizers. Essentially, the matrix-based BPMF performs the worst as the local temporal consistency is ignored. Tensor models like BGCP, BATE, and TF-ALS are slightly better than BPMF thanks to the global temporal consistency introduced by the "day" dimension. Our results suggest that BTMF (or BayesTRMF) inherits the advantages of both matrix models (e.g., TRMF and BPMF) and tensor models (e.g., BGCP, BATE, and TF-ALS): it not only provides a flexible and automatic inference technique for model parameter estimation, but also offers superior imputation performance by integrating temporal dynamics into matrix factorization.

We next conduct the experiment for making single-step and multi-step rolling predictions (see Figure 2) on the four data sets and Table 2 shows the performance of BTMF and other baseline models. As we can see, BTMF performs better than BayesTRMF and TRMF in most experiment. Although BayesTRMF is a fully Bayesian counterpart of TRMF, TRMF actually performs better than BayesTRMF in most cases. A possible reason is that TRMF uses both AR regularizer and F-norm penalty on temporal factors, while BayesTRMF only contains a prior on the AR process. With regard to BTMF, the prior of temporal factor is built on the VAR process which has better performance in characterizing the covariance

and causal structures. The comparison between BTMF and BayesTRMF clearly shows the the limitation of independent factor assumption in (4) and benefits of integrating VAR dynamics in (3).

As shown in Figure 5, our proposed BTMF achieves accurate time series prediction results on the Hangzhou metro passenger flow data set, and such accurate results can be guaranteed even with a large part of the input sequence is missing (for instance, see (c), (d), (f), and (h) of Figure 5). For Birmingham and Hangzhou data, Figure 6 gives the visualization on the prediction results achieved by BTMF on incomplete Birmingham parking data.

6.2 BTTF

Data set (N): NYC taxi⁵. This data set registers trip information (pick-up/drop-off locations and start time) for different types of taxi trips. For the experiment, we choose the trips collected during May and June 2018 (61 days) and organize the raw data into a third-order (pick-up zone \times drop-off zone \times time slot) tensor. We define in total 30 pick-up/drop-off zones and the temporal resolution for aggregating trips is selected as 1h. The size of this spatiotemporal tensor is $30 \times 30 \times 1464$.

Baselines. For imputation tasks, we select the Temporal Collaborative Filtering (TCF) technique—Bayesian Probabilistic Tensor Factorization (BPTF)—as a benchmark model [12]. Other baseline imputation models are BGCP, BATE, HaLRTC, and TF-ALS, which also have been selected above. In particular, we choose the Temporal Regularized Tensor Factorization (TRTF) as a baseline for both imputation and prediction tasks. In order to guarantee the TRTF's performance, we make cross validation carefully for the parameter tuning process. Moreover, we develop a Bayesian TRMF (BayesTRTF) for both two tasks.

Experiment setup. Similar to the analyses on BTMF, we also design two missing data scenarios: random missing (RM) by randomly removing entries in the tensor and non-random missing (NM) by randomly selecting pick-up \times drop-off \times day combinations and for each of them removing the corresponding 24h block entirely. We examine two missing rates (10% and 30%) and use the last seven days (i.e., 168 time slots) as the prediction period. For all of the competing models, their experiments are worked on the third-order tensor that comprised of pick-up zone, drop-off zone, and time slot.

Results and analysis. Table 3 shows the performance of competing models on both imputation and prediction tasks. Essentially, BTTF achieves competitive imputation results among these tensor models, and suggests smaller RMSEs in the single-step prediction task and competitive results in the multi-step prediction task. In the following, we give visualization results using BTTF for the single-step prediction. As an example, we depict the actual and predicted values for three randomly selected time series in Figure 8. Figure 7 shows examples of spatial volume at two time intervals. From these results, we can see that the temporal trend is well characterized by the BTTF model.

5. <https://www1.nyc.gov/site/tlc/about/tlc-trip-record-data.page>

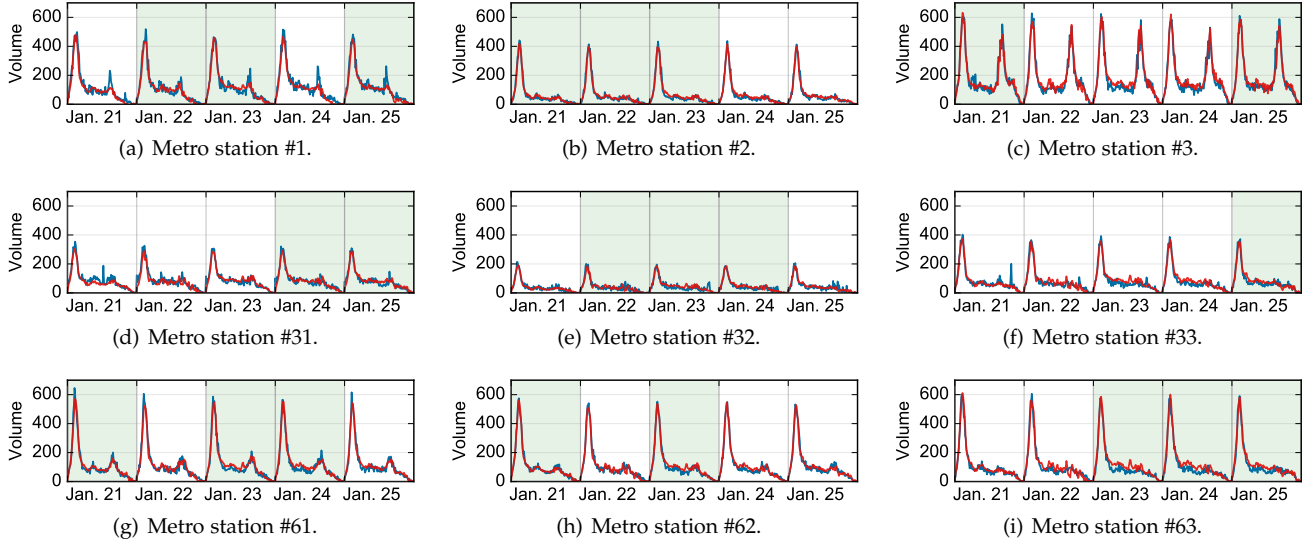


Fig. 5. Predicted metro passenger flow (i.e., red curves) of BTMF at 40% NM missing scenario vs. actual observations (i.e., blue curves). In these panels, white rectangles represent non-random missing (i.e., volume observations are lost in a whole day).

TABLE 3
Performance comparison on data set NYC taxi data (N).

		Original N	10%, RM	30%, RM	10%, NM	30%, NM
Missing data imputation	BTTF	-/-	51.98/ 4.66	51.78/4.77	52.65/ 4.75	52.71/4.90
	BayesTRTF	-/-	51.63/ 4.66	52.28/ 4.76	52.41/4.78	52.78/4.89
	TRTF	-/-	51.44/4.76	51.32/4.83	51.90/4.95	52.07/5.08
	BPTF	-/-	51.90/4.68	52.72/4.77	52.73/5.01	52.53/5.25
	BGCP	-/-	52.02/4.71	52.52/4.82	52.95/4.79	52.82/ 4.87
	BATF	-/-	60.37/4.94	62.62/5.09	62.02/5.04	60.85/5.02
	HaLRTC	-/-	49.29 /5.34	50.61 /6.31	50.01 /5.62	50.94 /6.59
	TF-ALS	-/-	52.62/6.24	54.88/6.90	51.70/5.99	-/-
Single-step prediction	BTTF	58.76/ 5.30	58.66/ 5.30	58.76/ 5.40	58.58/ 5.26	57.86/ 5.32
	BayesTRTF	58.16 /5.94	56.76/5.99	57.46 /6.09	59.17/5.98	57.25 /6.15
	TRTF	58.69/5.68	55.77 /5.78	59.09/6.20	55.60 /5.76	57.91/6.07
Multi-step prediction	BTTF	91.04/7.14	91.70/7.17	93.68/ 7.27	92.99/7.25	88.05/7.31
	BayesTRTF	86.48 /7.28	87.16/7.29	90.59/7.45	85.89 /7.40	86.51/7.46
	TRTF	86.87 / 7.13	86.79 / 7.14	87.40 /7.30	87.14 /7.18	86.04 /7.22

Best results are highlighted in bold fonts.

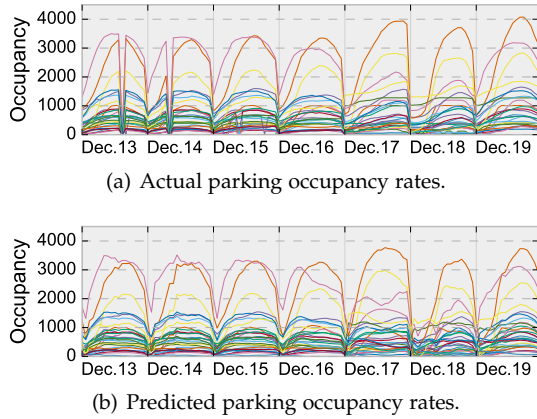


Fig. 6. Predicted occupancy of BTMF at 30% NM missing scenario vs. actual observations. Each curve corresponds to a car park.

7 CONCLUSION AND FUTURE WORK

In this paper we present a Bayesian Temporal Factorization (BTF) framework by incorporating a VAR layer into traditional Bayesian probabilistic MF/TF algorithms. The integration allows us to better model the complex temporal dynamics and covariance structure of multidimensional time series data on the latent dimension. Therefore, BTF provides a powerful tool to handle incomplete/corrupted time series data for both imputation and prediction tasks. The Bayesian scheme allows us to estimate the posterior distribution of target variables, which is critical to risk-sensitive applications. For model inference, we derive an efficient and scalable Gibbs sampling algorithm by introducing conjugate priors. The full Bayesian treatment offers additional flexibility in terms of parameter tuning and avoids overfitting issues. We examine the framework on several real-world time series matrices/tensors, and BTF framework has demonstrated superior performance over other baseline models. Although we introduce BTF in a

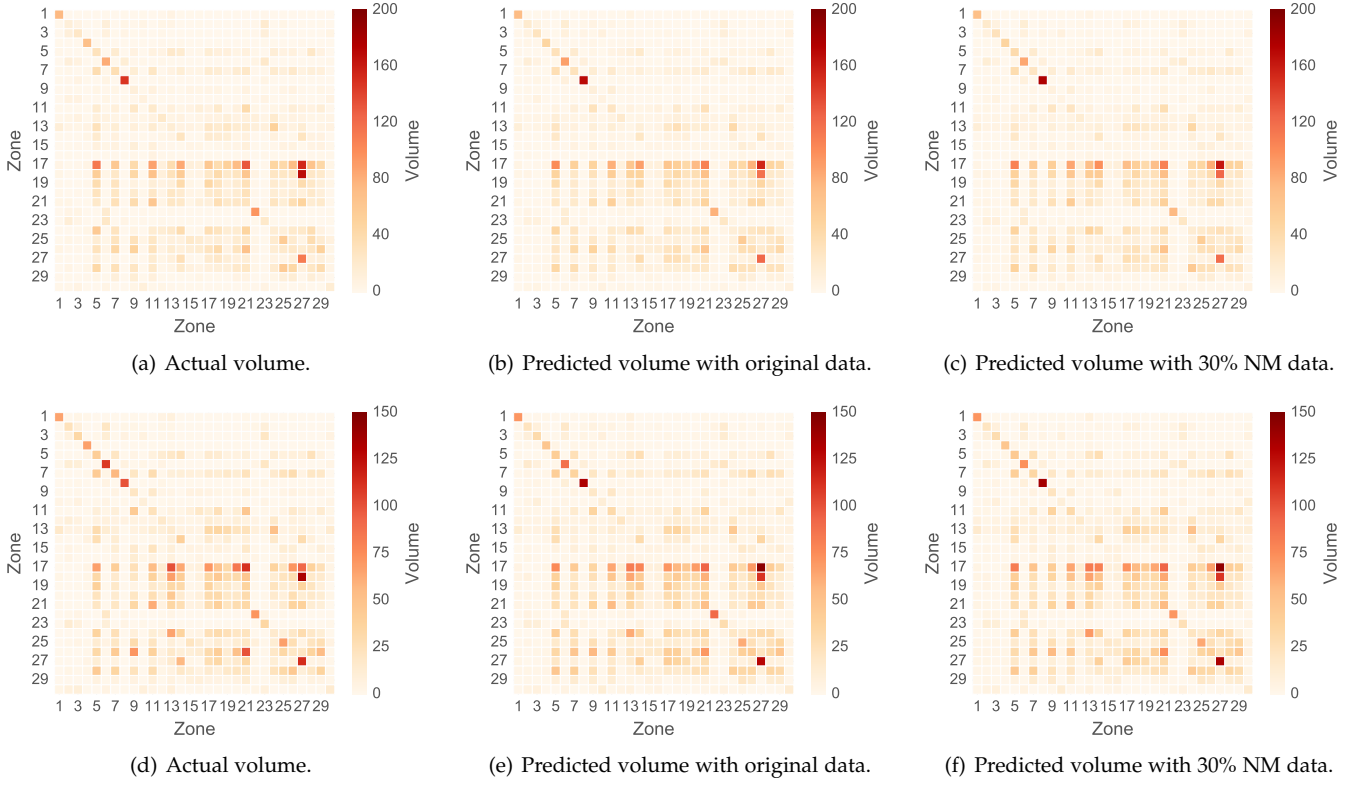


Fig. 7. Examples of volume at two time intervals. We show the predicted volume using BTTF with 30% NM and the actual observations. Note that above panels correspond to the time interval of 8:00 a.m. – 9:00 a.m. of June 27, and bottom panels correspond to the time interval of 9:00 a.m. – 10:00 a.m. of June 27.

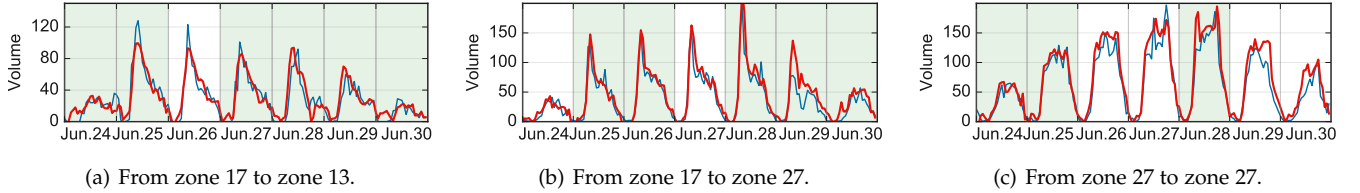


Fig. 8. Examples of three pick-up/drop-off pairs. We show the predicted time series using BTTF with 30% NM and the actual observations.

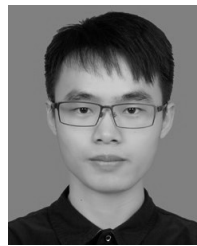
spatiotemporal setting, the model can be applied on general multidimensional time series data.

There are several directions to explore for future research. First, we will extend this framework to account for spatial dependencies/correlations by incorporating tools such as spatial AR and Laplacian kernels. Second, the graphical model can be further enhanced by accommodating exogenous variables and other distributions beyond Gaussian. Third, we would like to integrate recent advances in deep learning to better capture the complex and non-linear dynamics in modern time series data [39], [40], [41], [42], [43], [44], [45], [46].

REFERENCES

- [1] C. Faloutsos, J. Gasthaus, T. Januschowski, and Y. Wang, "Forecasting big time series: Old and new," *Proceedings of the VLDB Endowment*, vol. 11, no. 12, 2018.
- [2] X. Shi and D.-Y. Yeung, "Machine learning for spatiotemporal sequence forecasting: A survey," *arXiv preprint arXiv:1808.06865*, 2018.
- [3] Y. Li and C. Shahabi, "A brief overview of machine learning methods for short-term traffic forecasting and future directions," *SIGSPATIAL Special*, vol. 10, no. 1, pp. 3–9, 2018.
- [4] C. Chen, K. Petty, A. Skabardonis, P. Varaiya, and Z. Jia, "Freeway performance measurement system: mining loop detector data," *Transportation Research Record*, vol. 1748, no. 1, pp. 96–102, 2001.
- [5] P. Jing, Y. Su, X. Jin, and C. Zhang, "High-order temporal correlation model learning for time-series prediction," *IEEE Transactions on Cybernetics*, vol. 49, no. 6, pp. 2385–2397, 2018.
- [6] A. Schein, M. Zhou, D. Blei, and H. Wallach, "Bayesian poisson tucker decomposition for learning the structure of international relations," in *Proceedings of The 33rd International Conference on Machine Learning*, ser. Proceedings of Machine Learning Research, M. F. Balcan and K. Q. Weinberger, Eds., vol. 48. New York, New York, USA: PMLR, 20–22 Jun 2016, pp. 2810–2819.
- [7] R. Chen, D. Yang, and C.-h. Zhang, "Factor models for high-dimensional tensor time series," *arXiv preprint arXiv:1905.07530*, 2019.
- [8] L. Sun and K. W. Axhausen, "Understanding urban mobility patterns with a probabilistic tensor factorization framework," *Transportation Research Part B: Methodological*, vol. 91, pp. 511–524, 2016.
- [9] O. Anava, E. Hazan, and A. Zeevi, "Online time series prediction with missing data," in *International Conference on Machine Learning*, vol. 37, 2015, pp. 2191–2199.

- [10] Z. Che, S. Purushotham, K. Cho, D. Sontag, and Y. Liu, "Recurrent neural networks for multivariate time series with missing values," *Scientific Reports*, vol. 8, no. 1, p. 6085, 2018.
- [11] Z. Chen and A. Cichocki, "Nonnegative matrix factorization with temporal smoothness and/or spatial decorrelation constraints," *Laboratory for Advanced Brain Signal Processing, RIKEN, Tech. Rep.*, vol. 68, 2005.
- [12] L. Xiong, X. Chen, T.-K. Huang, J. Schneider, and J. G. Carbonell, "Temporal collaborative filtering with bayesian probabilistic tensor factorization," in *SIAM International Conference on Data Mining*, 2010, pp. 211–222.
- [13] M. Rogers, L. Li, and S. J. Russell, "Multilinear dynamical systems for tensor time series," in *Advances in Neural Information Processing Systems*, 2013, pp. 2634–2642.
- [14] M. T. Bahadori, Q. R. Yu, and Y. Liu, "Fast multivariate spatio-temporal analysis via low rank tensor learning," in *Advances in neural information processing systems*, 2014, pp. 3491–3499.
- [15] T. V. Nguyen, E. V. Bonilla et al., "Collaborative multi-output Gaussian processes," in *Uncertainty in Artificial Intelligence (UAI)*, 2014, pp. 643–652.
- [16] W. Sun and D. Malioutov, "Time series forecasting with shared seasonality patterns using non-negative matrix factorization," in *Advances in Neural Information Processing Systems (NIPS) Time Series Workshop*, 2015.
- [17] Y. Cai, H. Tong, W. Fan, P. Ji, and Q. He, "Facets: Fast comprehensive mining of coevolving high-order time series," in *Proceedings of the 21th ACM SIGKDD International Conference on Knowledge Discovery and Data Mining*. ACM, 2015, pp. 79–88.
- [18] D. Deng, C. Shahabi, U. Demiryurek, L. Zhu, R. Yu, and Y. Liu, "Latent space model for road networks to predict time-varying traffic," in *Proceedings of the 22nd ACM SIGKDD International Conference on Knowledge Discovery and Data Mining*. ACM, 2016, pp. 1525–1534.
- [19] H.-F. Yu, N. Rao, and I. S. Dhillon, "Temporal regularized matrix factorization for high-dimensional time series prediction," in *Advances in Neural Information Processing Systems*, 2016, pp. 847–855.
- [20] K. Takeuchi, H. Kashima, and N. Ueda, "Autoregressive tensor factorization for spatio-temporal predictions," in *IEEE International Conference on Data Mining*, 2017, pp. 1105–1110.
- [21] B. Hooi, K. Shin, S. Liu, and C. Faloutsos, "Smf: Drift-aware matrix factorization with seasonal patterns," in *Proceedings of the 2019 SIAM International Conference on Data Mining*. SIAM, 2019, pp. 621–629.
- [22] M. Araujo, P. Ribeiro, H. A. Song, and C. Faloutsos, "Tensorcast: forecasting and mining with coupled tensors," *Knowledge and Information Systems*, vol. 59, no. 3, pp. 497–522, 2019.
- [23] F. Han, H. Lu, and H. Liu, "A direct estimation of high dimensional stationary vector autoregressions," *The Journal of Machine Learning Research*, vol. 16, no. 1, pp. 3115–3150, 2015.
- [24] Z. Ghahramani and G. E. Hinton, "Parameter estimation for linear dynamical systems," Technical Report CRG-TR-96-2, University of Toronto, Dept. of Computer Science, Tech. Rep., 1996.
- [25] R. Chen, H. Xiao, and D. Yang, "Autoregressive models for matrix-valued time series," *arXiv preprint arXiv:1812.08916*, 2018.
- [26] J. Z. Sun, D. Parthasarathy, and K. R. Varshney, "Collaborative kalman filtering for dynamic matrix factorization," *IEEE Transactions on Signal Processing*, vol. 62, no. 14, pp. 3499–3509, 2014.
- [27] C. Xie, A. Talk, and E. Fox, "A unified framework for missing data and cold start prediction for time series data," in *Advances in Neural Information Processing Systems (NIPS) Time Series Workshop*, 2016.
- [28] K. D. Harris, A. Aravkin, R. Rao, and B. W. Brunton, "Time-varying autoregression with low rank tensors," *arXiv preprint arXiv:1905.08389*, 2019.
- [29] H. Tan, Y. Wu, B. Shen, P. J. Jin, and B. Ran, "Short-term traffic prediction based on dynamic tensor completion," *IEEE Transactions on Intelligent Transportation Systems*, vol. 17, no. 8, pp. 2123–2133, 2016.
- [30] R. Salakhutdinov and A. Mnih, "Bayesian probabilistic matrix factorization using markov chain monte carlo," in *International Conference on Machine Learning*, 2008, pp. 880–887.
- [31] Q. Zhao, L. Zhang, and A. Cichocki, "Bayesian CP factorization of incomplete tensors with automatic rank determination," *IEEE Transactions on Pattern Analysis and Machine Intelligence*, vol. 37, no. 9, pp. 1751–1763, 2015.
- [32] X. Chen, Z. He, Y. Chen, Y. Lu, and J. Wang, "Missing traffic data imputation and pattern discovery with a Bayesian augmented tensor factorization model," *Transportation Research Part C: Emerging Technologies*, vol. 104, pp. 66–77, 2019.
- [33] L. Charlin, R. Ranganath, J. McInerney, and D. M. Blei, "Dynamic poisson factorization," in *Proceedings of the 9th ACM Conference on Recommender Systems*, 2015, pp. 155–162.
- [34] S. Karlsson, "Forecasting with bayesian vector autoregression," in *Handbook of Economic Forecasting*, ser. Handbook of Economic Forecasting, G. Elliott and A. Timmermann, Eds. Elsevier, 2013, vol. 2, pp. 791–897.
- [35] S. Gultekin and J. Paisley, "Online forecasting matrix factorization," *IEEE Transactions on Signal Processing*, vol. 67, no. 5, pp. 1223–1236, March 2019.
- [36] T. G. Kolda and B. W. Bader, "Tensor decompositions and applications," *SIAM Review*, vol. 51, no. 3, pp. 455–500, 2009.
- [37] X. Chen, Z. He, and L. Sun, "A Bayesian tensor decomposition approach for spatiotemporal traffic data imputation," *Transportation Research Part C: Emerging Technologies*, vol. 98, pp. 73–84, 2019.
- [38] J. Liu, P. Musialski, P. Wonka, and J. Ye, "Tensor completion for estimating missing values in visual data," *IEEE Transactions on Pattern Analysis and Machine Intelligence*, vol. 35, no. 1, pp. 208–220, 2013.
- [39] A. Ghaderi, B. M. Sanandaji, and F. Ghaderi, "Deep forecast: Deep learning-based spatio-temporal forecasting," *arXiv preprint arXiv:1707.08110*, 2017.
- [40] R. Yu, S. Zheng, A. Anandkumar, and Y. Yue, "Long-term forecasting using tensor-train rnns," *arXiv preprint arXiv:1711.00073*, 2017.
- [41] J. Zhang, Y. Zheng, and D. Qi, "Deep spatio-temporal residual networks for citywide crowd flows prediction," in *AAAI Conference on Artificial Intelligence*, 2017, pp. 1655–1661.
- [42] W. Cao, D. Wang, J. Li, H. Zhou, L. Li, and Y. Li, "Brits: Bidirectional recurrent imputation for time series," in *Advances in Neural Information Processing Systems*, 2018, pp. 6775–6785.
- [43] Y. Liang, S. Ke, J. Zhang, X. Yi, and Y. Zheng, "Geoman: Multi-level attention networks for geo-sensory time series prediction," in *Proceedings of the 27th International Joint Conference on Artificial Intelligence*, 2018, pp. 3428–3434.
- [44] S. S. Rangapuram, M. W. Seeger, J. Gasthaus, L. Stella, Y. Wang, and T. Januschowski, "Deep state space models for time series forecasting," in *Advances in Neural Information Processing Systems*, 2018, pp. 7785–7794.
- [45] B. Yu, H. Yin, and Z. Zhu, "Spatio-temporal graph convolutional networks: a deep learning framework for traffic forecasting," in *Proceedings of the 27th International Joint Conference on Artificial Intelligence*, 2018, pp. 3634–3640.
- [46] Y. Wang, A. Smola, D. Maddix, J. Gasthaus, D. Foster, and T. Januschowski, "Deep factors for forecasting," in *International Conference on Machine Learning*, 2019, pp. 6607–6617.



Xinyu Chen received the B.S. degree in Traffic Engineering from Guangzhou University, Guangzhou, China, in 2016, and M.S. degree in Transportation Engineering from Sun Yat-Sen University, Guangzhou, China, in 2019. His current research centers on spatiotemporal data modeling, machine learning, and intelligent transportation systems, and he works closely with Prof. Lijun Sun on these fields.



Lijun Sun received the B.S. degree in Civil Engineering from Tsinghua University, Beijing, China, in 2011, and Ph.D. degree in Civil Engineering (Transportation) from National University of Singapore in 2015. He is currently an Assistant Professor with the Department of Civil Engineering and Applied Mechanics at McGill University, Montreal, QC, Canada. His research centers on intelligent transportation systems, machine learning, spatiotemporal modeling, travel behavior, and agent-based simulation.